Diversity-Multiplexing Tradeoff in Rank-Deficient and Spatially Correlated MIMO Channels

Woohyuk Chang, Sae-Young Chung, and Yong H. Lee
Dept. of EECS, Korea Advanced Institute of Science and Technology, Daejeon, Korea
Email: whchang@stein.kaist.ac.kr, sychung@ee.kaist.ac.kr, yohlee@ee.kaist.ac.kr

Abstract— In this paper, we first generalize a recent work of Zheng and Tse on diversity-multiplexing tradeoff (DMT) for some rank-deficient channels (poor scattering). We show that rank deficiency lowers DMT curves from that of i.i.d. Rayleigh fading channels. We show an interesting observation that suggests a fractional diversity gain may be possible at integer multiplexing gains. As the scattering becomes rich, the DMT approaches that of the i.i.d. Rayleigh fading channels.

We next focus on spatially correlated multiple-input multiple-output (MIMO) channels. We show that spatial correlation does not change the DMT but still degrades the outage performance and analyze such a degradation at high SNR.

I. INTRODUCTION

Increasing demands for higher data rate and more reliable communication have motivated adopting multiple antennas at transmitters and receivers [1], [2]. MIMO can be used to provide the diversity gain (increasing reliability of reception) or to provide the multiplexing gain (increasing data rate or degrees of freedom). Recent work of Zheng and Tse [3] characterized a fundamental tradeoff between diversity and multiplexing gains in MIMO channels. More recently, Azarian and El Gamal [4] introduced a new notion called the throughput-reliability tradeoff (TRT) where they explain other aspects which cannot be captured by Zheng and Tse's diversity-multiplexing tradeoff (DMT) such as how diversity gain changes as SNR increases for a fixed rate, and how much the required SNR increases as rate increases for a fixed probability of error.

In [5]–[11], MIMO channels are modeled assuming various scattering conditions and array configurations that can cause rank deficiency in MIMO channels and spatial correlation among antennas. In this paper, we focus on degradation of the DMT caused by such more realistic environments. In [12], the DMT and asymptotic behaviors of the outage are analyzed for MIMO Rician channels and channels with partial channel state information at the transmitter. We first consider two types of rank-deficient channel models. We show that DMT curves for the rank-deficient channels are lowered from that of the i.i.d. Rayleigh fading channels. In [13], it is shown that relays can be used as active scatterers to make the scattering environment more rich. We verify that as the scattering becomes rich, the DMT curves are improved and approach to that of the i.i.d. Rayleigh fading channels. We finally consider spatial

correlation in MIMO channels based on the Kronecker model [6], [14], [15]. It is shown that the degradation caused by spatial correlation cannot be captured by the DMT since the degradation appears only as a penalty in SNR gap in dB. We analyze such a gap at high SNR.

The rest of the paper is organized as follows. Section II presents a brief review on DMT and TRT. In Section III, we explain the two types of rank-deficient channel models and evaluate their DMT curves. Section IV is devoted to spatially correlated MIMO channels.

II. A BRIEF REVIEW ON DMT AND TRT

We consider a MIMO channel with m transmit and n receive antennas. The fading path gain h_{ij} from the jth transmit antenna to the ith receive antenna is assumed to be zero-mean circular-symmetric complex Gaussian with unit variance known only at the receiver, but not at the transmitter. We also assume that the path gains are slowly varying such that h_{ij} stays fixed during a block of l symbols. We denote the transmitted (received) signal from the ith transmit (receive) antenna by x_i (y_i), respectively. Then, the received signal at n receive antennas at any given time during a block of l symbols is

$$\boldsymbol{y} = \sqrt{\frac{\rho}{m}} \boldsymbol{H} \boldsymbol{x} + \boldsymbol{W} \qquad (1)$$

where $\boldsymbol{H} = [h_{ij}] \in \mathbb{C}^{n \times m}$, $\boldsymbol{x} = [x_i] \in \mathbb{C}^m$, $\boldsymbol{W} = [w_i] \in \mathbb{C}^n$, $\boldsymbol{y} = [y_i] \in \mathbb{C}^n$, $\boldsymbol{H}$ and $\boldsymbol{W}$ have i.i.d. entries $h_{ij} \sim \mathcal{CN}(0, 1)$ and $w_i \sim \mathcal{CN}(0, 1)$, and ρ is the average SNR at each receive antenna.

In [3], Zheng and Tse defined multiplexing gain r and diversity gain d as

$$\lim_{\rho \to \infty} \frac{R}{\log \rho} = r \qquad (2)$$

and

$$\lim_{\rho \to \infty} \frac{\log P_e(R, \rho)}{\log \rho} = -d, \qquad (3)$$

where R and $P_e(R, \rho)$ are achievable data rate and probability of error of a family of codes. Throughout the paper, we assume logarithms are to the base 2. They considered the best achievable diversity gain $d^*(r)$ for a given r, and found that $d^*(r)$ for the i.i.d. Rayleigh fading MIMO channels when

$l \geq m + n - 1$ is given as the piecewise linear function with corner points given by

$$d^*(r) = (m - r)(n - r) \quad (4)$$

for integers $r \leq \min\{m, n\}$.

In [4], Azarian and El Gamal refined the DMT results of [3] to show a tradeoff between increased throughput and decreased probability of error as SNR increases. Specifically, for $k \in \mathbb{Z}$ and $0 \leq k < \min\{m, n\}$, the outage probability P_o for a constant rate transmission can be characterized by

$$\lim_{\rho \to \infty, \, R \in \mathcal{R}(k)} \frac{\log P_o(R, \rho) - c(k)R}{\log \rho} = -g(k) \quad (5)$$

and

$$\lim_{\rho \to \infty, R > \min\{m, n\}\log \rho} \frac{\log P_o(R, \rho)}{\log \rho} = 0, \quad (6)$$

where

$$c(k) \triangleq m + n - (2k + 1),$$
$$g(k) \triangleq mn - k(k + 1),$$
$$\mathcal{R}(k) \triangleq \left\{ R \,\middle|\, k < \frac{R}{\log \rho} < k + 1 \right\}, \quad (7)$$

and

$$P_o \triangleq \inf_{p(\boldsymbol{x})} \Pr\left\{ H \in \mathbb{C}^{n \times m} \,\middle|\, I(\boldsymbol{x}; \boldsymbol{y}|\boldsymbol{H} = H) < R \right\}. \quad (8)$$

Similar can be said about P_e [4]. They showed that the slope of the outage curve for a fixed rate is given by $-g(k)$, and the horizontal spacing in dB between two outage curves with a rate difference of ΔR is given by $3\Delta R c(k)/g(k)$.

In this paper, we estimate the diversity gain $d^*(k)$ numerically and derive an upper bound on $d^*(k)$ analytically.

III. DMT FOR RANK-DEFICIENT CHANNELS

In this section, we evaluate the DMT for two types of rank-deficient channel models.

A. Poor scattering environment

We consider the rank-deficient MIMO channel model in a poor scattering environment as shown in Fig 1. Scatterers are located far from both the transmitter and the receiver, and grouped into P clusters where there are K scatterers in each cluster. The distance between the transmitter (or receiver) and each cluster is assumed to be large enough so that the angular spread of the path from the transmitter (or receiver) to each cluster is vanishingly small. Then, the channel gain $\boldsymbol{H}_p$ from transmit antennas to receive antennas through the p-th cluster can be modeled as

$$\boldsymbol{H}_p = \boldsymbol{u}_p \cdot h_p \cdot \boldsymbol{v}_p^\dagger \quad (9)$$

where $\boldsymbol{u}_p$ and $\boldsymbol{v}_p$ are the column vectors whose elements are i.i.d. complex random variables uniform on the unit circle. We consider two extreme cases of $K \to \infty$ and $K = 1$. As $K \to \infty$, h_p is approximated as a complex Gaussian random variable (Rayleigh fading). If $K = 1$, then h_p is deterministic. We assume that path-losses are same for all paths to simplify

analysis, i.e., $\mathbb{E}\{|h_p|^2\} = 1$ is the same for all p. Note that there can exist dependency among the elements of $\boldsymbol{u}_p$ and $\boldsymbol{v}_p$, but we assume that they are independent. We also assume that $\boldsymbol{u}_p$, $\boldsymbol{v}_p$, and h_p are independent for all p. Then, the channel gain $\boldsymbol{H}$ assuming P clusters is given by

$$\boldsymbol{H} = \frac{1}{\sqrt{P}} \sum_{p=1}^{P} \boldsymbol{H}_p = \frac{1}{\sqrt{P}} \sum_{p=1}^{P} \boldsymbol{u}_p \cdot h_p \cdot \boldsymbol{v}_p^\dagger \quad (10)$$

whose rank is upper bounded by $\min\{P, m, n\}$. Note that even if the scattering is poor, the rank can be artificially increased by using relays as active scatterers [13]. Although scatterers are not considered to be grouped into several clusters in [9], the resultant expression for the channel matrix $\boldsymbol{H}$ of the finite scatterers model in [9] is identical to (10). If time delays among paths are same in the random matrix model [10], then it is same as the case of $K = 1$ in (10).

We first consider the case of $K \to \infty$. Fig. 2 shows, for example, two outage curves with a rate difference of 2 for a 2×2 rank-deficient MIMO channel with P clusters. If we increase the data rate by 2, the difference of the two curves in SNR becomes 3 dB in the upper part of Fig. 2 ($k = 1$), i.e., the multiplexing gain is 2, where the corresponding diversity gain $d^*(2)$ is 0. The difference of the two curves in SNR becomes 6 dB on the boundary of the two regions $k = 0$ and $k = 1$, i.e., the multiplexing gain is 1, where $d^*(1)$ is $\Delta/6$ and Δ is the change in $10 \log_{10} P_o$. Note that if the multiplexing gain is 0, the corresponding diversity gain $d^*(0)$ becomes just the slope of the curve for rate R in the lower part ($k = 0$). In the rest of this section, we show how to obtain Δ (and thus the DMT) for the rank-deficient MIMO channel model in (10).

Fig. 3 shows that our simulation results on the slope $\frac{\partial \log P_o}{\partial \log \rho}$ for $R = 4, 8, 12, 16, 20,$ and 24 in 2×2 rank-deficient channels when $P = 2$. We can see that the slope corresponding to $R = 24$ is sharply decreasing until about -0.8, near which it is decreasing slowly, and again sharply decreasing until about -1.8. This decreasing tendency of the slope can be interpreted as follows. From the TRT analysis in [4], the slope for a fixed R is expected to be $-g(k)$ for ρ satisfying $R \in \mathcal{R}(k)$ and abruptly changing into $-g(k - 1)$ when ρ increases such that $R \in \mathcal{R}(k-1)$. The first interval where the slope for $R = 24$ is sharply decreasing from 0 to -0.8 corresponds to the boundary of $\mathcal{R}(2)$ and $\mathcal{R}(1)$ in the TRT analysis. The interval near -0.8 and -1.8 corresponds to the region of $k = 1$ and $k = 0$, respectively. It is interesting to observe fractional diversity gains.

Since we have $g(2) = 0$, $g(1) = 0.8$, and $g(2) = 1.8$ based on Fig. 3, $d^*(k)$ can also be estimated similarly as shown in Fig. 2. For example, $d^*(1) = \Delta/6 = 3g(1)/6 = 0.4$. Table I and Fig. 4 (a) show $g(k)$ and $d^*(k)$ for $P = 1, 2, 3$ and 10. When $P = 1$, the DMT curve is same as that of single-input single-output (SISO) Rayleigh fading channels. We can see that as P increases, the estimated DMT curves approach that of the i.i.d. Rayleigh fading MIMO channels since the scattering becomes rich as P increases. In Fig. 4 (a), the estimated DMT curves are always lower than that of the i.i.d. $\boldsymbol{H}$. Although

we considered the case of $m = n = 2$, this method can be applied to other m and n.

For the special case of $\min\{m, n\} = 2$, we find the following upper bound for the DMT as shown in Fig. 4 (b).

Theorem 1: For the rank-deficient Rayleigh fading ($K \to \infty$) MIMO channels in (10) with $\min\{m, n\} = 2$ and P clusters, the optimal tradeoff curve $d^*(r)$ is upper bounded by lower of the following two piecewise-linear functions. One is given by connecting the points $(r, d^*(r))$ where

$$d^*(0) = P, \ d^*(1) = \frac{P-1}{2}, \ \text{and} \ d^*(2) = 0. \tag{11}$$

The other is given by connecting the points $(r, d^*(r))$ where

$$d^*(r) = (m - r)(n - r), \ r = 0, 1, 2. \tag{12}$$

Proof: We refer readers to the full paper [16]. ∎

For the rank-deficient Rayleigh fading ($K \to \infty$) MIMO channels in (10) with P clusters, the optimal tradeoff curve $d^*(r)$ in the limit of $m, n \to \infty$ is given by

$$d^*(r) = P - r, \tag{13}$$

where $0 \le r \le P$ as shown in Fig. 5 (a).

For given m, n and $K = 1$, we consider two extreme cases of $P = 1$ and $P \to \infty$. For $P = 1$, this channel model is equivalent to AWGN channel. As $P \to \infty$, it is equivalent to the i.i.d. Rayleigh fading MIMO channel. Hence, the DMT curves for these cases are shown in Fig. 5 (b).

There is a slightly different rank-deficient model called the keyhole model [7], [8]. In [17], the DMT of a double scattering model is characterized, and hence that of the keyhole model can be easily found as its special case. For the $m \times n$ keyhole model, the optimal tradeoff curve $d^*(r)$ is given by

$$d^*(r) = \min\{m, n\}(1 - r), \tag{14}$$

where $0 \le r \le 1$.

Note that as m and n increase, the DMT curve of the keyhole model is improved, but that of the rank-deficient model in (10) with $P = 1$ and $K \to \infty$ does not change. Two DMT curves coincide only when $\min\{m, n\} = 1$.

B. Forcing some eigenvalues to zero

Although not physically motivated as the one in Section III-A, the following model provides an alternative model for rank-deficient channels. Rank deficiency in a channel matrix can be introduced directly by just forcing some eigenvalues of $\boldsymbol{H}\boldsymbol{H}^\dagger$ to zero.

Theorem 2: If randomly chosen $n - k$ eigenvalues of $\boldsymbol{H}\boldsymbol{H}^\dagger$ are forced to zero in the $m \times n$ MIMO channel $\boldsymbol{H} = [h_{ij}]$, $h_{ij} \sim \mathcal{CN}(0, 1)$ with $m \ge n$, the optimal tradeoff curve is same as that of the $(m + n - k) \times k$ MIMO channel $\boldsymbol{G} = [g_{ij}]$, $g_{ij} \sim \mathcal{CN}(0, 1)$.

Proof: We refer readers to the full paper [16]. ∎

We can get the same result by the following intuitive approach. If for the full rank MIMO channel $\boldsymbol{H}$, the multiplexing gain is k, then its number of complex dimensions reduces from mn to $mn - (m - k)(n - k)$, and the reduced number of dimensions $(m - k)(n - k)$ is the diversity gain. If we force

$n - k$ eigenvalues of $\boldsymbol{H}\boldsymbol{H}^\dagger$ to zero, the rank of $\boldsymbol{H}$ is k and its dimension is $mn - (m - k)(n - k)$. For this rank-deficient channel, let r denote the multiplexing gain. In this case, we can also get the diversity gain from calculating the reduced number of dimensions. Since the dimension is reduced from $mn - (m - k)(n - k)$ to $mn - (m - r)(n - r)$, the reduced number of dimensions is

$$
\begin{aligned}
& mn - (m - k)(n - k) - \{mn - (m - r)(n - r)\} \\
= \ & mk + nk - k^2 - mr - nr + r^2 \\
= \ & (m + n - k - r)(k - r),
\end{aligned}
\tag{15}
$$

which is same as the diversity gain of $(m + n - k) \times k$ MIMO channels with full rank.

IV. SPATIALLY CORRELATED MIMO CHANNELS

Since the space at the mobile station is usually limited, we cannot have many antennas and furthermore correlation among them is unavoidable. On the other hand, there are enough space at the base station to implement many antennas with enough separation. Under this practical consideration, we assume that the signals are correlated only at one site where the number of antennas is less than or equal to that at the other site. For example, if $n \le m$, the correlation exists only among the receive antennas.

When there exists a spatial correlation among the receive antennas, the columns of $\boldsymbol{H}$ are independent, but the elements of each column are correlated [6], [14], [15]. We denote the jth column of $\boldsymbol{H}$ by $\boldsymbol{h}_j = (h_{1j}, h_{2j}, \cdots, h_{nj})^T$, where we assume $\mathbb{E}\{\boldsymbol{h}_j\} = \boldsymbol{0}$ and the correlation matrix $\boldsymbol{\Sigma} = \mathbb{E}\{\boldsymbol{h}_j\boldsymbol{h}_j^\dagger\}$ is the same for $j = 1, \cdots, m$. Then, $\boldsymbol{H}$ can be represented by

$$\boldsymbol{H} = \boldsymbol{\Sigma}^{\frac{1}{2}}\boldsymbol{H}_w \tag{16}$$

where $\boldsymbol{H}_w$ is the i.i.d. Rayleigh fading MIMO channel [6], [14], [15]. Similarly, the spatial correlation among the transmit antennas makes the rows of $\boldsymbol{H}$ be independent, but the elements of each row are correlated.

Since the optimal input covariance matrix that maximizes the outage capacity for nonergodic fading channels is still unknown, we take the input distribution as Gaussian with a covariance matrix $\boldsymbol{Q}$. In [3], the upper and the lower bounds for the outage probability are derived by choosing $\boldsymbol{Q} = \boldsymbol{I}_m$ and $\boldsymbol{Q} = m\boldsymbol{I}_m$, respectively. Such choices of $\boldsymbol{Q}$ are valid regardless of the distribution of $\boldsymbol{H}$. We first show that the DMT is not affected by the correlation.

Lemma 1: For the $m \times n$ correlated MIMO channel with correlation matrix $\boldsymbol{\Sigma}$, the optimal tradeoff curve $d^*(r)$ is same as that of $\boldsymbol{\Sigma} = \boldsymbol{I}$.

Proof: See the Appendix A. ∎

Fig. 6 shows the lower bound on the outage probability P_o in 2×2 MIMO channels for rate $R = 24$ where three cases with correlation and one case without ($\boldsymbol{\Sigma} = \boldsymbol{I}$) are considered. The correlation is specified by the ordered eigenvalues $\sigma_1 \le \sigma_2$ of $\boldsymbol{\Sigma}$, i.e., $(\sigma_1, \sigma_2) = (0.1, 1.9)$, $(0.3, 1.7)$, and $(0.9, 1.1)$. We can see that the degradation appears only as a penalty in SNR gap in dB, and such a gap depends on the eigenvalues

of $\boldsymbol{\Sigma}$. Hence, the DMT and the TRT are not changed by the spatial correlation. The only thing worth being evaluated here is the amount of such a gap.

Theorem 3: For the $m \times n$ MIMO channel with correlation matrix $\boldsymbol{\Sigma}$, if

$$c = |\boldsymbol{\Sigma}|^{-\frac{1}{\min\{m,n\}}}, \qquad (17)$$

then

$$\lim_{\rho \to \infty} \frac{P_o^{(\gamma)}(R, \rho c, \boldsymbol{\Sigma})}{P_o^{(\gamma)}(R, \rho, \boldsymbol{I})} = 1, \qquad (18)$$

where

$$P_o^{(\gamma)}(R, \rho c, \boldsymbol{\Sigma}) = \Pr\left\{\log \det\left(I_n + \frac{\rho c}{\gamma} HH^\dagger\right) < R\right\} \quad (19)$$

Proof: See the Appendix B. ∎

Note that $P_o^{(\gamma)}(R, \rho c, \boldsymbol{\Sigma})$ is the lower (upper) bound of $P_o(R, \rho c, \boldsymbol{\Sigma})$ when $\gamma = 1$ ($\gamma = m$), respectively. This prediction is well matched by simulation as shown in Fig. 6. Specifically, the predicted SNR gaps are 3.61 dB, 1.46 dB, and 0.63 dB for $(\sigma_1, \sigma_2) = (0.1, 1.9)$, $(0.3, 1.7)$, and $(0.9, 1.1)$, respectively, which are close to the measured SNR gaps 3.5 dB, 1.3 dB, and 0.4 dB, respectively.

APPENDIX

We provide only a sketch of proofs due to lack of space.

A. Proof of Lemma 1

For the $m \times n$ correlated MIMO channel with correlation matrix $\boldsymbol{\Sigma}$, the joint pdf of ordered eigenvalues $\lambda_1 \leq \cdots \leq \lambda_{\min\{m,n\}}$ of $\boldsymbol{HH}^\dagger$ (or $\boldsymbol{H}^\dagger \boldsymbol{H}$) is given by [18], [19]

$$p(\boldsymbol{\lambda}) = K_{m,n}^{-1} |\boldsymbol{\Sigma}|^{-M} \prod_{i=1}^N \lambda_i^{M-N} \prod_{i<j}^N (\lambda_i - \lambda_j)^2 \, {}_0\tilde{F}_0\left(-\boldsymbol{\Sigma}^{-1}, \mathbf{W}\right),$$

where

$${}_0\tilde{F}_0\left(-\boldsymbol{\Sigma}^{-1}, \mathbf{W}\right) = \frac{\prod_{i=1}^N (i-1)! \, |\boldsymbol{E}(\boldsymbol{\lambda}, \boldsymbol{\sigma})|}{\prod_{j<i}(\lambda_i - \lambda_j) \prod_{j<i}(-\frac{1}{\sigma_i} + \frac{1}{\sigma_j})}, \quad (20)$$

$M = \max\{m, n\}$, $N = \min\{m, n\}$, $\boldsymbol{E}(\boldsymbol{\lambda}, \boldsymbol{\sigma}) = \left[e^{-\frac{\lambda_j}{\sigma_i}}\right] \in \mathbb{C}^{N \times N}$, and $\sigma_1 \leq \cdots \leq \sigma_N$ are the ordered eigenvalues of $\boldsymbol{\Sigma}$. Since $|\boldsymbol{E}(\boldsymbol{\lambda}, \boldsymbol{\sigma})|$ can be expanded as

$$|\boldsymbol{E}(\boldsymbol{\lambda}, \boldsymbol{\sigma})| = \frac{\prod_{j<i}(\lambda_i - \lambda_j) \prod_{j<i}(-\frac{1}{\sigma_i} + \frac{1}{\sigma_j})}{\prod_{i=1}^N (i-1)!}(1 + O(\lambda_n)),$$

we have

$$p(\boldsymbol{\lambda}) = K_{m,n}^{-1} |\boldsymbol{\Sigma}|^{-M} \prod_i \lambda_i^{|m-n|} \prod_{i<j}(\lambda_i - \lambda_j)^2$$
$$\times (1 + O(\lambda_n)) \qquad (21)$$

which provides the same DMT curve as that of the i.i.d. Rayleigh fading channels.
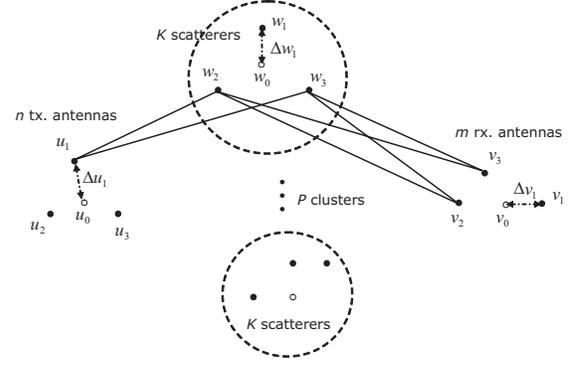
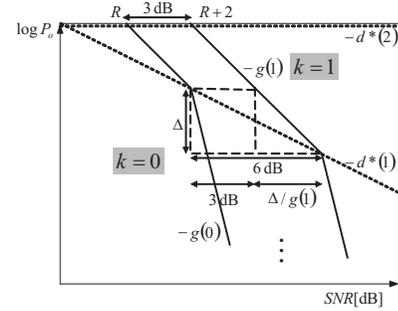

Fig. 1. Rank-deficient MIMO channel model.

Fig. 2. Two outage curves with a rate difference of 2.

B. Proof of Theorem 3

From (21), $P_o^{(\gamma)}(R, \rho c, \boldsymbol{\Sigma})$ in (19) is written by

$$P_o^{(\gamma)}(R, \rho c, \boldsymbol{\Sigma}) = \int_{\mathcal{A}(R, \rho c)} K_{m,n}^{-1} |\boldsymbol{\Sigma}|^{-\max\{m,n\}}$$
$$\times \prod_{i=1}^N \lambda_i'^{|m-n|} \prod_{i<j}(\lambda_i' - \lambda_j')^2 (1 + O(\lambda_n')) \, d\boldsymbol{\lambda}' \qquad (22)$$

where $\mathcal{A}(R, \rho c) = \left\{\boldsymbol{\lambda}' \left| \log\left(\prod_{i=1}\left(1 + \frac{\rho c}{\gamma}\lambda_i'\right)\right) < R\right.\right\}$. Letting $\lambda_i = c\lambda_i'$, we get

$$P_o^{(\gamma)}(R, \rho c, \boldsymbol{\Sigma}) = \int_{\mathcal{A}(R, \rho)} K_{m,n}^{-1} c^{-mn} |\boldsymbol{\Sigma}|^{-\max\{m,n\}}$$
$$\times \prod_{i=1}^N \lambda_i^{|m-n|} \prod_{i<j}(\lambda_i - \lambda_j)^2 (1 + O(\lambda_n)) \, d\boldsymbol{\lambda}. \quad (23)$$

Therefore, we get

$$\frac{P_o^{(\gamma)}(R, \rho c, \boldsymbol{\Sigma})}{P_o^{(\gamma)}(R, \rho, \boldsymbol{I})} = c^{-mn} |\boldsymbol{\Sigma}|^{-\max\{m,n\}}$$
$$\times \frac{\int_{\mathcal{A}(R,\rho)} \prod_i \lambda_i^{|m-n|} \prod_{i<j}(\lambda_i - \lambda_j)^2 (1 + O(\lambda_n)) \, d\boldsymbol{\lambda}}{\int_{\mathcal{A}(R,\rho)} \prod_i \lambda_i^{|m-n|} \prod_{i<j}(\lambda_i - \lambda_j)^2 (1 + O(\lambda_n)) \, d\boldsymbol{\lambda}},$$

which means that if we choose $c = |\boldsymbol{\Sigma}|^{-\frac{1}{\min\{m,n\}}}$, then

$$\lim_{\rho \to \infty} \frac{P_o^{(\gamma)}(R, \rho c, \boldsymbol{\Sigma})}{P_o^{(\gamma)}(R, \rho, \boldsymbol{I})} = c^{-mn} |\boldsymbol{\Sigma}|^{-\max\{m,n\}} = 1. \qquad (24)$$
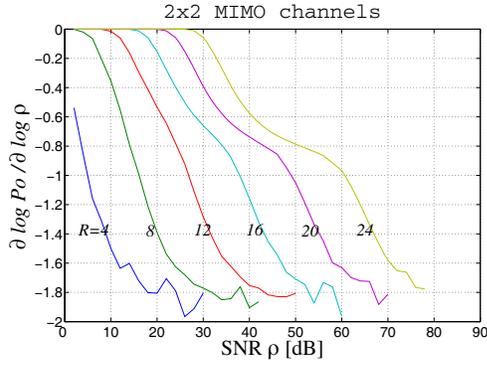
Fig. 3. Slopes of the outage probabilities for 2×2 rank-deficient Rayleigh fading MIMO channels when $P = 2$.
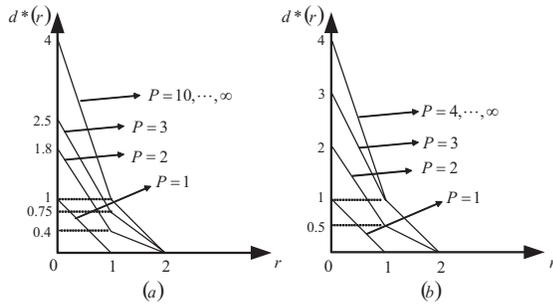

Fig. 4. DMT for 2×2 rank-deficient Rayleigh fading ($K \to \infty$) MIMO channels (exact for $P = 1$ and $P = \infty$): (a) estimated; (b) upper bound.
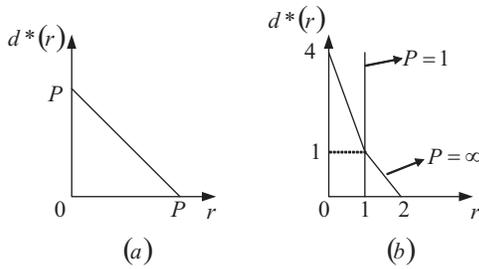

Fig. 5. DMT for rank-deficient MIMO channels: (a) $K \to \infty$ (Rayleigh fading) and $m, n \to \infty$; (b) $m = n = 2$ and $K = 1$.

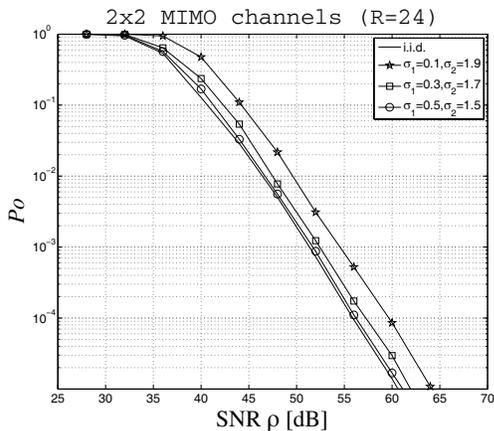Fig. 6. The outage probability P_o in 2×2 MIMO channels for rate $R = 24$.

TABLE I

ESTIMATED $g(k)$ AND $d^*(k)$ FOR 2×2 RANK-DEFICIENT RAYLEIGH FADING MIMO CHANNELS (EXACT FOR $P = 1$ AND $P = \infty$)

P	$g(1)$	$d^*(1)$	$g(0) = d^*(0)$
1	0	0	1
2	0.8	0.4	1.8
3	1.5	0.75	2.5
10	2	1	4
∞	2	1	4

REFERENCES

[1] G. J. Foschini and M. J. Gans, "On limits of wireless communications in a fading environment when using multiple antennas," *Wireless Personal Commun.*, vol. 6, pp. 311–335, Mar. 1998.

[2] V. Tarokh, N. Seshadri, and A. R. Calderbank, "Space-time codes for high data rate wireless communications: Performance criterion and code construction," *IEEE Trans. Inform. Theory*, vol. 44, pp. 744–765, Mar. 1998.

[3] L. Zheng and D. N. C. Tse, "Diversity and multiplexing: A fundamental tradeoff in multuple-antenna channels," *IEEE Trans. Inform. Theory*, vol. 49, pp. 1073–1096, May 2003.

[4] K. Azarian and H. El Gamal, "The throughput-reliability tradeoff in MIMO channels," *IEEE Trans. Inform. Theory*, submitted for publication.

[5] G. G. Raleigh and J. M. Cioffi, "Spatio-temporal coding for wireless communication," *IEEE Trans. Commun.*, vol. 46, pp. 357–366, Mar. 1998.

[6] D.-S. Shiu, G. J. Foschini, M. J. Gans, and J. M. Kahn, "Fading correlation and its effect on the capacity of multielement antenna systems," *IEEE Trans. Commun.*, vol. 48, pp. 502–513, Mar. 2000.

[7] D. Gesbert, H. Bölcskei, D. A. Gore, and A. J. Paulraj, "Outdoor MIMO wireless channels: Models and performance prediction," *IEEE Trans. Commun.*, vol. 50, pp. 1926–1934, Dec. 2002.

[8] D. Chizhik, G. J. Foschini, M. J. Gans, and R. A. Valenzuela, "Keyholes, correlations, and capacities of multielement transmit and receive antennas," *IEEE Trans. Wireless Commun.*, vol. 1, pp. 361–368, Apr. 2002.

[9] A. G. Burr, "Capacity bounds and estimates for the finite scatterers MIMO wireless channel," *IEEE J. Select. Areas Commun.*, vol. 21, pp. 812–818, June 2003.

[10] R. R. Müller, "A random matrix model of communication via antenna arrays," *IEEE Trans. Inform. Theory*, vol. 48, pp. 2495–2506, Sept. 2002.

[11] A. S. Y. Poon, D. N. C. Tse, and R. W. Brodersen, "Impact of scattering on the capacity, diversity, and propagation range of multiple-antenna channels," *IEEE Trans. Inform. Theory*, vol. 52, pp. 1087–1100, Mar. 2006.

[12] W.-Y. Shin, S.-Y. Chung, and Y. H. Lee, "Outage analysis for MIMO Rician channels and channels with partial CSI," in *Proc. IEEE Int. Symp. Inform. Theory (ISIT)*, 2006.

[13] A. Wittneben and B. Rankov, "Impact of cooperative relays on the capacity of rank-deficient MIMO channels," in *Proc. 12th IST Summit on Mobile and Wireless Commun.*, June 2003, pp. 421–425.

[14] C.-N. Chuah, D. N. C. Tse, J. M. Kahn, and R. A. Valenzuela, "Capacity scaling in MIMO wireless systems under correlated fading," *IEEE Trans. Inform. Theory*, vol. 48, pp. 637–650, Mar. 2002.

[15] M. Chiani, M. Z. Win, and A. Zanella, "On the capacity of spatially correlated MIMO Rayleigh-fading chennels," *IEEE Trans. Inform. Theory*, vol. 49, pp. 2363–2371, Oct. 2003.

[16] W. Chang, S.-Y. Chung, and Y. H. Lee, "Diversity-multiplexing tradeoff in rank-deficient and spatially correlated MIMO channels," in preparation.

[17] S. Yang and J.-C. Belfiore, "Diversity-multiplexing tradeoff of double scattering MIMO channels," *IEEE Trans. Inform. Theory*, submitted for publication.

[18] A. T. James, "Distributions of matrix variates and latent roots derived from normal samples," *Ann. Math. Statist.*, vol. 35, pp. 475–501, 1964.

[19] C. G. Khatri, "On the moments of traces of two matirces in three situations for complex multivariate normal populations," *Sankhya, The Indian J. Statist., Ser. A*, vol. 32, pp. 65–80, 1970.